

Mechanisms of DNA Binding and Regulation of *Bacillus anthracis* DNA Primase[†]

Subhasis B. Biswas,* Eric Wydra, and Esther E. Biswas

Department of Molecular Biology, University of Medicine and Dentistry of New Jersey, Stratford, New Jersey 08084

Received January 20, 2009; Revised Manuscript Received June 29, 2009

ABSTRACT: DNA primases are pivotal enzymes in chromosomal DNA replication in all organisms. In this article, we report unique mechanistic characteristics of recombinant DNA primase from *Bacillus anthracis*. The mechanism of action of *B. anthracis* DNA primase (DnaG_{BA}) may be described in several distinct steps as follows. Its mechanism of action is initiated when it binds to single-stranded DNA (ssDNA) in the form of a trimer. Although DnaG_{BA} binds to different DNA sequences with moderate affinity (as expected of a mobile DNA binding protein), we found that DnaG_{BA} bound to the origin of bacteriophage G4 (G4ori) with approximately 8-fold higher affinity. DnaG_{BA} was strongly stimulated (≥ 75 -fold) by its cognate helicase, DnaB_{BA}, during RNA primer synthesis. With the G4ori ssDNA template, DnaG_{BA} formed short (≤ 20 nucleotides) primers in the absence of DnaB_{BA}. The presence of DnaB_{BA} increased the rate of primer synthesis. The observed stimulation of primer synthesis by cognate DnaB_{BA} is thus indicative of a positive effector role for DnaB_{BA}. By contrast, *Escherichia coli* DnaB helicase (DnaB_{EC}) did not stimulate DnaG_{BA} and inhibited primer synthesis to near completion. This observed effect of *E. coli* DnaB_{EC} is indicative of a strong negative effector role for heterologous DnaB_{EC}. We conclude that DnaG_{BA} is capable of interacting with DnaB proteins from both *B. anthracis* and *E. coli*; however, between DnaB proteins derived from these two organisms, only the homologous DNA helicase (DnaB_{BA}) acted as a positive effector of primer synthesis.

Chromosomal DNA replication in *Escherichia coli* requires many proteins and enzymes that work in unison to execute the initiation, elongation, and termination stages of DNA synthesis (1–3). At the origin of *E. coli* replication, *oriC*, DnaA protein initiates the process through localized melting of the origin and subsequent recruitment of other replication proteins to form a large nucleoprotein complex (4–6). DnaB protein joins the DnaA·*oriC* complex and unwinds the duplex DNA at the partially melted origin. The entry of DnaB protein at *oriC* requires the complex formation of DnaB protein with DnaC protein. The DNA binding activity of DnaB is enhanced by its association with DnaC; by contrast, its ATPase activity is attenuated (7–10). With the help of DnaA, DnaC guides DnaB to the DnaA·*oriC* complex.

In the replication of *E. coli* RK2 plasmid DNA, DnaA plays a similar role in delivering the DnaB·DnaC complex to the replication origin of the RK2 plasmid and activating the helicase activity with plasmid-encoded TrfA protein (11–13). Incidentally, during the replication of bacteriophage λ , the phage-encoded λ P protein binds to DnaB protein, shuts off its ATPase activity, and guides it to the activated λ origin (8, 14, 15). The activated λ origin is created by phage-encoded λ O protein (the functional equivalent of DnaA protein) binding to the λ origin (14–17). A comparison of the two replication systems clearly indicates that DnaB protein plays a crucial role in determining the fate of replication at each origin (8). The presence of DnaB

protein appears to be sufficient for other replication proteins such as primase and DNA polymerase III holoenzyme¹ to follow and join the complex afterward.

After DnaC or λ P protein departs from the origin complex, DnaG primase is recruited to the replication fork through a transient protein–protein interaction with DnaB in the origin (5). Unlike the holoenzyme, DnaG can initiate and elongate short RNA primers, which are then extended by the holoenzyme (18–21). DnaG synthesizes RNA primer or primes only once to initiate leading strand DNA synthesis. However, it must prime repeatedly on the lagging strand, and these primers lead to the synthesis of Okazaki fragments (22). It has been demonstrated that primase initiates in vivo Okazaki fragment synthesis of *E. coli* chromosome and G4 bacteriophage. Initiation predominantly occurs from unique regions containing CTG trinucleotide (20, 21). DNA primases are very specific in choosing priming sites during the initiation event, but its specificity is reduced significantly in the presence of DnaB, which allows the primase to synthesize multiple primers on the lagging strand of the replication fork (18). Kinetic analysis suggests that *E. coli* primase acting alone is the slowest RNA polymerase with an in vitro rate of approximately one primer per second, which may be accelerated by the addition of DnaB protein (19, 21, 23, 24). It is thus highly likely that formation of the DnaB·DnaG complex triggers lagging strand primer synthesis.

[†]This work was supported in part by grants from the National Institutes of Allergy and Infectious Diseases (AI064974), the UMDNJ Foundation, and a Summer Medical Research Fellowship Grant to E.W. (MSII) from the UMDNJ Foundation.

*To whom correspondence should be addressed: Department of Molecular Biology, University of Medicine and Dentistry of New Jersey, Stratford, NJ 08084. Telephone: (856) 566-6270. Fax: (856) 566-6291. E-mail: subhasis.biswas@umdnj.edu.

¹Abbreviations: holoenzyme, DNA polymerase III holoenzyme; ssDNA, single-stranded DNA; G4ori, origin of bacteriophage G4; EMSA, electrophoretic mobility shift assay; DTT, dithiothreitol; TBE, Tris-Borate-EDTA buffer; SDS, sodium dodecyl sulfate; PAGE, polyacrylamide gel electrophoresis; rNTP, ribonucleotide triphosphate; DnaG_{BA}, DNA primase of *Bacillus anthracis*; DnaB_{BA}, DnaB helicase of *B. anthracis*; DnaG_{EC}, DNA primase of *Escherichia coli*; DnaB_{EC}, DnaB helicase of *E. coli*.

In the *E. coli* replication fork, primase acts distributively; for example, the frequency of primer synthesis increases with the concentration of primase (25, 26). The average length of the Okazaki fragments decreases correspondingly because the length of the Okazaki fragments is inversely proportional to the frequency of primer synthesis. Primase binding to a ssDNA template may therefore play an important role in both the rate and extent of primer synthesis. Even though primase exists primarily as a monomer in solution, we have previously shown that it forms a multimeric primase·DNA complex in the absence of DnaB_{EC} (20, 21).

Despite the well-known diversity among prokaryotic organisms, studies on DNA replication in prokaryotes generally have focused only on *E. coli* and its bacteriophages. *E. coli* is a Gram-negative bacterium; however, most of the emerging pathogens are Gram-positive, and the DNA replication process in this class of prokaryotes remains poorly understood (27). It is possible that the replication enzymes and proteins in Gram-positive prokaryotes would have characteristics significantly different from those found in *E. coli*. The genomes of a large number of Gram-positive pathogens, including *Bacillus anthracis*, have been completely sequenced (28, 29). Though it is still not possible to grow these bacteria in large scale and purify their replication proteins, biochemical analysis of their replication processes is now feasible because of the ability to clone and express their individual replication protein components. Previous studies of Gram-positive DNA primase from *Staphylococcus aureus* were hampered due to the fact that recombinant protein expressed by *E. coli* is completely insoluble and can be studied as only a glutathione *S*-transferase (GST) fusion protein with a large GST appendage (30, 31). In contrast to *E. coli* primase, DNA primase purified from the high-temperature bacterium *Bacillus stearothermophilus* (DnaG_{BS}) appears to form a stable complex with its cognate DnaB_{BS} (32). This complex contains three DnaG_{BS} molecules per DnaB hexamer. Bailey et al. resolved the X-ray structure of a complex of DnaB_{BS} with the helix binding domain of DnaG_{BS} at 2.9 Å resolution, and it demonstrated that the two proteins formed a complex with a 6:3 ratio (33).

This study demonstrates that the replicative DNA primase from Gram-positive bacteria exhibits novel mechanisms of action, rarely observed for other classes of bacterial primases.

MATERIALS AND METHODS

Nucleic Acids, Enzymes, Oligonucleotides, and Other Reagents. Ultrapure ribonucleotides were obtained from GE Biosciences (Piscataway, NJ) and were used without further purification. [α -³²P]UTP was obtained from Perkin-Elmer Inc. (Boston, MA). All other chemicals used to prepare buffers and solutions were reagent grade and were purchased from Fisher Chemical Co. (Pittsburgh, PA). Ion exchange resins (POROS-Q and POROS-S) were from Applied Biosystems Inc. (Foster City, CA). The preparative HPLC gel filtration column (Bio-Sil TSK250, 21.5 mm × 60 cm) was obtained from Bio-Rad Inc. (Hercules, CA) and was used in a Biocad 20 HPLC system from Applied Biosystems Inc. The analytical HPLC gel filtration column (7.8 mm × 30 cm) was from Tosoh Biosciences LLC (Montgomeryville, PA).

Buffers. Lysis buffer consisted of 25 mM Tris-HCl (pH 7.9), 10% sucrose, and 250 mM NaCl. Buffer A consisted of 25 mM Tris-HCl (pH 7.5), 5 mM MgCl₂, 10% glycerol, 5 mM DTT, and NaCl as indicated. Buffer B consisted of 20 mM Tris-HCl

(pH 7.5), 5 mM MgCl₂, 10% glycerol, and KCl as indicated. The following oligonucleotides were used: G4ori, 5'-GCCGTCCCT-ACTGCAAAGCCAAAAGGA-3'; Fl-G4ori, 5'-FAM-GCCG-TCCCTACTGCAAAGCCAAAAGGA-3'; Sixtymer, 5'-GGG-GTCTCACGACGTTGTAAAACGACTGCAGCCGTTGT-CGAGCTCGGTACCC GGGGTAGGA-3'.

Cloning and Expression of DnaG_{BA}. The DnaG_{BA} gene was amplified by PCR using genomic DNA from *B. anthracis* strain 9131, obtained as a gift from T. M. Koehler of the University of Texas Houston Health Science Center (Houston, TX) (28). This ORF encodes a 598-amino acid polypeptide with a predicted molecular mass of 68.3 kDa. The amplified gene was inserted into a pET30a vector (Novagen Inc., Madison, WI) under the control of a T7 promoter (pET30a-DnaG_{BA} recombinant plasmid).

Purification of DnaG_{BA}. DnaG_{BA} was purified from the *E. coli* BL21(DE3)RIL strain (Stratagene Inc., La Jolla, CA) harboring the pET30a-DnaG_{BA} plasmid. *E. coli* cells were grown in 8 L batches in 2×YT medium containing 50 µg/mL kanamycin and 12 µg/mL chloramphenicol at 37 °C to an OD₆₀₀ of 0.4–0.6, and 1-isopropyl 1-thio- β -D-galactopyranoside (IPTG) was added to a final concentration of 0.25 mM. The cells were grown for an additional 12 h at 12–13 °C and then harvested by centrifugation at 8000 rpm for 10 min at 4 °C. The cell pellet was resuspended in lysis buffer [25 mM Tris-HCl (pH 7.9) and 10% sucrose] and frozen at –80 °C, until further use. Cells were thawed on ice, adjusted to pH 8.0 with 1 M Tris base, and lysed using 0.25 mg/mL lysozyme and 5 mM MgCl₂, 5 mM spermidine·HCl, and 2.5 mM DTT via incubation on ice for 60 min. This is followed by a 5 min incubation at 37 °C. The mixture was homogenized on ice followed by centrifugation. The lysate was centrifuged at 19000 rpm for 30 min at 4 °C. The supernatant was precipitated overnight using 0.25 g/mL ammonium sulfate on ice followed by centrifugation. The precipitate was collected by centrifugation at 18000 rpm for 30 min at 4 °C. The protein pellet was resuspended in buffer A (fraction II).

DnaG_{BA} protein was first purified by POROS-Q anion exchange chromatography (Applied Biosystems Inc.). The salt concentration of DnaG_{BA} fraction II was adjusted to the conductivity of buffer A₂₅ (buffer A with 25 mM NaCl) by dilution with buffer A₀. The protein was then passed through a 5 mL POROS-Q column equilibrated with buffer A₂₅. DnaG_{BA} protein was eluted with a 100 mL gradient from A₂₅ to A₃₀₀. The DnaG_{BA} fractions, identified by SDS–PAGE, were pooled (fraction III) and bound to a 5 mL POROS-S column equilibrated with buffer A₁₀₀. DnaG_{BA} protein was eluted with a gradient of buffers A₁₀₀ and A₅₀₀. The fractions were analyzed by SDS–PAGE. The DnaG_{BA}-containing fractions were pooled and concentrated by ultrafiltration using a Millipore YM30 membrane. Finally, it was purified to homogeneity by HPLC gel filtration using a Bio-Rad TSK gel filtration column (2.1 cm × 60 cm). Purified DnaG_{BA} was ≥99% pure. Protein homogeneity was determined by SDS–PAGE.

RNA Primer Synthesis Assay. RNA primer synthesis was conducted essentially as described by Stayton and Kornberg (21), with minor modifications. Briefly, the typical 25 µL reaction mixture contained 20 mM Tris-HCl (pH 7.5), 8 mM dithiothreitol (DTT), 4% (w/v) glycerol, 80 µg/mL bovine serum albumin, 8 mM MgCl₂, GTP and CTP (each at 100 µM), 0.5 mM ATP, 20 µM UTP, 0.125 µCi of [α -³²P]UTP, and 5 pmol of ssDNA template with enzymes as indicated. Samples were incubated at 30 °C for 15 min unless otherwise indicated. Reactions were

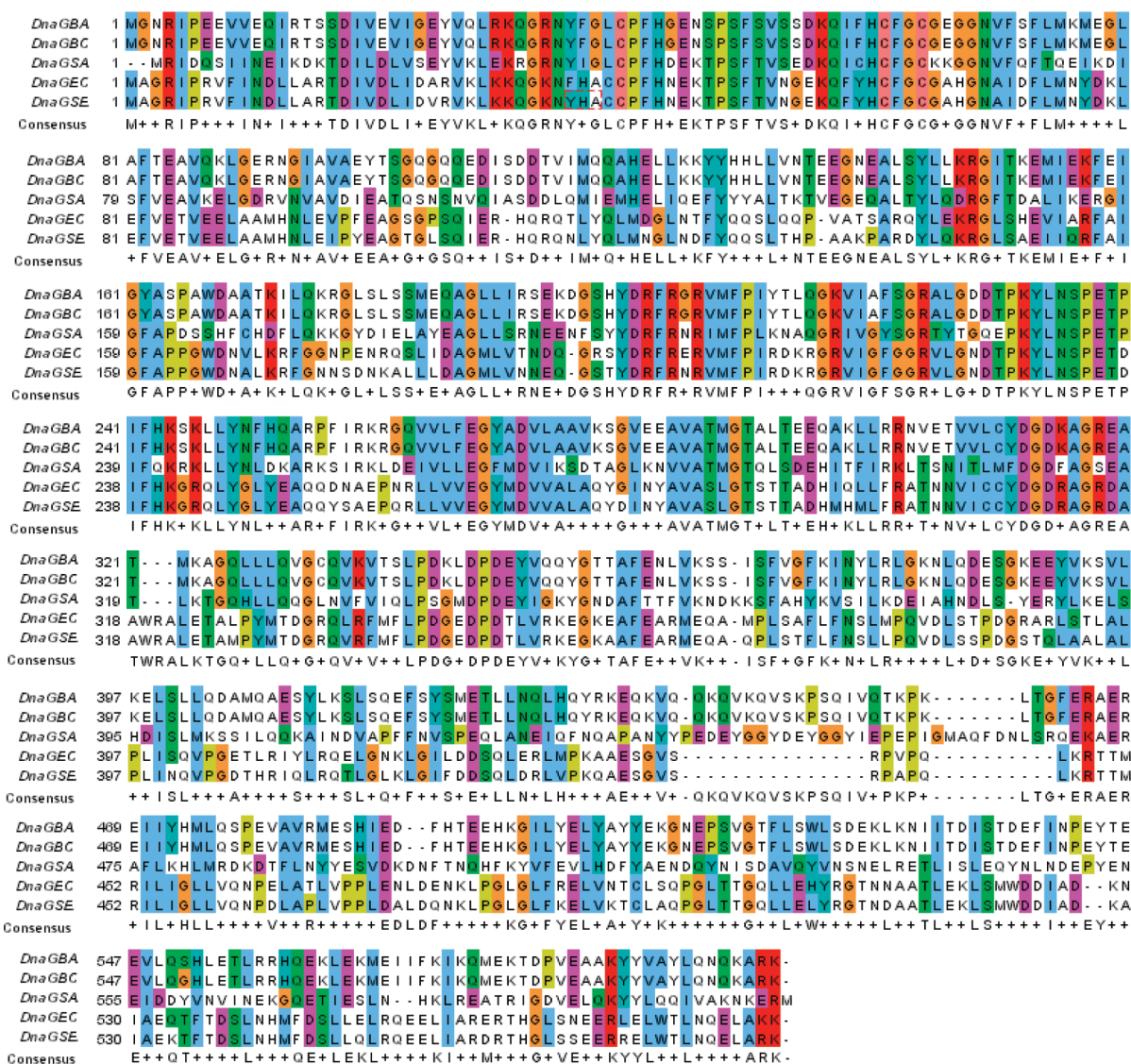


FIGURE 1: Sequence homology of DNA primases. DnaG proteins from *B. anthracis* (DnaGBA), *B. cereus* (DnaGBC), *St. aureus* (DnaGSA), *E. coli* (DnaGEC), and *S. enterica* (DnaGSE) were aligned, and motifs were identified using the CLUSTALW2 program of the InterProScan Web site (<http://www.ebi.ac.uk/Tools/InterProScan/>). The color coding is as follows: red, basic; blue, hydrophobic; green, hydrophilic; orange, neutral; pink, acidic; and light green, proline.

stopped when the mixtures were chilled on ice and purified by being passed through a micro gel filtration column. Purified primed template was ethanol precipitated with 40 μ g of glycogen and 3 volumes of 100% ethanol and incubated at -80°C . Pellets were air-dried and resuspended in 8 μ L of formamide loading buffer (95% formamide, 20 mM EDTA, 0.01% bromophenol blue, and 0.01% xylene cyanol).

RNA Primer Analysis. RNA primers were analyzed by denaturing polyacrylamide gel electrophoresis. Samples were heated at 95°C for 2 min and loaded immediately onto a 20% polyacrylamide sequencing gel (15 cm \times 50 cm, 0.4 mm thick) containing 7 M urea and 1 \times TBE [89 mM Tris-borate (pH 8.3) and 2.5 mM EDTA]. Electrophoresis was conducted for 4 h at 55 W in 1 \times TBE buffer. Gels were dried and exposed to Fuji RX film at -80°C for 12–24 h.

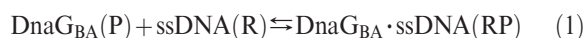
Electrophoretic Mobility Shift DNA Binding Assay (EMSA). An EMSA was conducted as described previously (19, 34). Briefly, reactions were conducted in a 25 μ L final volume of binding buffer [25 mM Tris-HCl (pH 7.5), 10% (v/v) glycerol, 0.1 mg/mL BSA, 10 mM MgCl_2 , and 5 mM DTT] containing

200 pg of ^{32}P -labeled oligonucleotide, 100 ng of poly(dI-dC), and protein as indicated. The binding reactions were allowed to proceed for the specified time, after which 2 μ L of 0.1% bromophenol blue in loading buffer was added. A fraction (85%) of the reaction mixtures was immediately loaded onto a 4 to 8% polyacrylamide gel containing 1 \times TBE. Electrophoresis was conducted at 30 mA; the gel was dried and autoradiographed. Band quantitations were conducted by scintillation counting.

Steady-State Anisotropy Measurement. Equilibrium DNA binding in solution was assessed by fluorescence anisotropy (35–37). Fluorescence measurements were performed on a steady-state photon counting spectrofluorometer, PC1, from ISS Instruments (Champaign, IL) equipped with a Hamamatsu R928P photomultiplier tube. Excitation and emission slits were adjusted at 8 and 4 nm, respectively.

Fluorescein-labeled G4ori oligonucleotide, Fl-G4ori, was used as a fluorescence anisotropy probe. The oligonucleotide was diluted in buffer B to a concentration of 6 nM and titrated with DnaGBA in the concentration range of 0.1 nM to 1 μ M. The

samples were excited at 488 nm, and the fluorescence anisotropy was measured at 540 nm (38), where minimal variation in the total fluorescence intensity was observed. Fluorescence intensities were measured for 3×10 s and averaged. Anisotropy values were expressed as millianisotropy (mA), which is equal to the anisotropy divided by 1000. The standard deviation for the anisotropy values was < 5 mA. The total fluorescence intensity did not change significantly with an increase in protein concentration. Therefore, fluorescence lifetime changes or the scattered excitation light did not affect anisotropy measurements. The interaction of DnaG_{BA} with labeled oligonucleotide can be represented as follows:



where R is the ligand, i.e., fluorescently labeled oligonucleotide, and P is the protein or DnaB_{BA} in this case. As shown previously (39), the equilibrium dissociation constant, K_d , can be further defined as the DnaB_{BA} concentration at which half of the ssDNA molecules are in the protein–DNA complex.

DNA Binding Data Analysis. The anisotropy protein titration data or EMSA data were fitted to eq 2 using nonlinear regression analysis. The data points were fitted to an equation for a sigmoidal semilogarithmic plot using Prism 5.0 (GraphPad Software Inc.) presented in eq 2.

$$Y = Y_{\min} + (Y_{\max} - Y_{\min}) / [1 + 10^{(\log EC_{50} - X)N_{\text{app}}}] \quad (2)$$

where Y represents the value of DNA binding, Y_{\min} and Y_{\max} are the values at the bottom and top plateaus of the plots, respectively, EC_{50} is the X value (or enzyme concentration) at 50% DNA binding (or K_d), and N_{app} is the Hill coefficient, which represents the number of molecules of protein (DnaG_{BA}) bound to a single molecule of ssDNA or the composition of the DnaG_{BA}·ssDNA complex.

RESULTS

DNA Primase Gene of *B. anthracis*. The DNA primase gene of *B. anthracis* (BAS4195) was identified by BLAST search of the annotated sequenced genome of *B. anthracis* Stern (28, 29). BAS4195 was the only gene in the *B. anthracis* genome that is homologous to the *E. coli* *dnaG* gene. The gene encodes a polypeptide of 598 amino acid residues with a deduced molecular mass of 68.3 kDa.

Significant Homology Was Observed in the N-Terminus of DnaG_{BA}. The amino acid sequence of the polypeptide was compared with the sequences of a number of Gram-positive (*Bacillus cereus* and *St. aureus*) and Gram-negative (*E. coli* and *Salmonella enterica*) DNA primases. Multiple-sequence alignment of these sequences is shown in Figure 1. Extensive homology of DnaG_{BA} was observed within the family of DNA primases from Gram-positive bacteria and to a lesser degree with the Gram-negative primases. Overall, high degrees of homology were observed in three regions (Figure 1). All three of these regions are located at the N-terminus: amino acid residues 1–320, which constitute the major part of the primase core domain with 25% identity and 45% similarity; amino acid residues 1–80, where the zinc-finger domain is located (residues 5–103) which displayed ~36% identity and 35% similarity. A second area of homology was observed between residues 186 and 254 with 41% identity and ~41% similarity. A third area of homology was observed between residues 264 and 320 with 25% identity and ~49% similarity.

Unlike the case in the N-terminus of primase, homology in the C-terminus between amino acid residues 321 and 599 was rather minimal and there were significant gaps in some of the sequences, particularly in the Gram-negative sequences. Interestingly, DnaG_{SA} of *St. aureus* contained a unique seven-amino acid insertion starting at residue 459 (Figure 1) that was not present in any of the other primases discussed here. The C-terminus of primase is known to be involved in the interaction with its cognate DnaB helicase, and this interaction is pivotal in the efficient and rapid priming of the lagging strand of the replication fork as well as movement of the replisome (40–42). Thus, the lack of homology in this region could help explain the specificity of the helicase–primase interaction. A motif search indicated that a putative DnaB helicase binding domain (or helicase binding motif) in DnaG_{BA} is located at amino acids 466–591. Homology in this domain among these five DnaG proteins is significantly low: 5% identity and ~20% similarity (Figure 1). Therefore, it is likely that the lack of homology in the C-terminal domain among bacterial primases makes the interaction species-specific for cognate primase–helicase pairs. Although this assumption is logical, it has not been rigorously examined.

Anthrax Primase, DnaG_{BA}, Is Monomeric in Solution.

Previous attempts to purify DNA primase from Gram-positive bacteria, *St. aureus* (DnaG_{SA}), led to a protein that is insoluble. It is soluble only as a glutathione *S*-transferase (GST) fusion protein, and removal of the GST moiety leads to the precipitation of cleaved primase (30). Studies with GST–DnaG_{SA} fusion protein showed a lack of stimulation with cognate DnaB protein (30, 31). Interestingly, our earlier attempts to purify DnaG_{BA} as a His₆ fusion protein using Ni²⁺ affinity chromatography also produced an inactive protein (data not shown). Therefore, to understand the mechanism of action of Gram-positive DNA primases, we needed to purify it in its native form without any modification of its polypeptide sequence.

Therefore, we expressed DnaG_{BA} in its native polypeptide sequence, without any N- or C-terminal fusion, in *E. coli*. Surprisingly, unmodified recombinant DnaG_{BA}, expressed in *E. coli*, was highly soluble, unlike that observed with other DnaG_{SA} forms. Because of its high solubility, it could be purified by a simple combination of chromatographic procedures. The final stage in the purification was high-performance gel filtration chromatography (Figure 2A). This step removed all of the remaining impurities. It should also be noted that whenever a recombinant protein (like DnaG_{BA}) is overexpressed, often some aggregated proteins are produced during expression and purification. The aggregates copurify with the target protein in ion exchange columns and, in general, cannot be distinguished via SDS–PAGE. In HPLC gel filtration, the aggregated proteins fractionate in the void volume (> 300 kDa), which is the case here [fractions 30–34 (Figure 2A)]. The aggregated form of DnaG_{BA} did not have any enzymatic activity and, therefore, was not pursued further. Thus, HPLC gel filtration completely separated purified biologically active primase [major peak, fractions 40–46 (Figure 2A)] from impurities as well as aggregated proteins. Since we were studying the oligomeric state of DnaG_{BA} in formation of the DNA–protein complex, it was important to determine that the preparation was free from aggregated protein. SDS–PAGE analysis of the purified active DnaG_{BA} indicated approximately ~99% purity (Figure 3C). This DnaG_{BA} peak eluted from the column at an elution volume that is similar to that of BSA (68 kDa). Thus, DnaG_{BA} appeared to be a monomer in solution. The protein fractions were first assayed by an EMSA using a

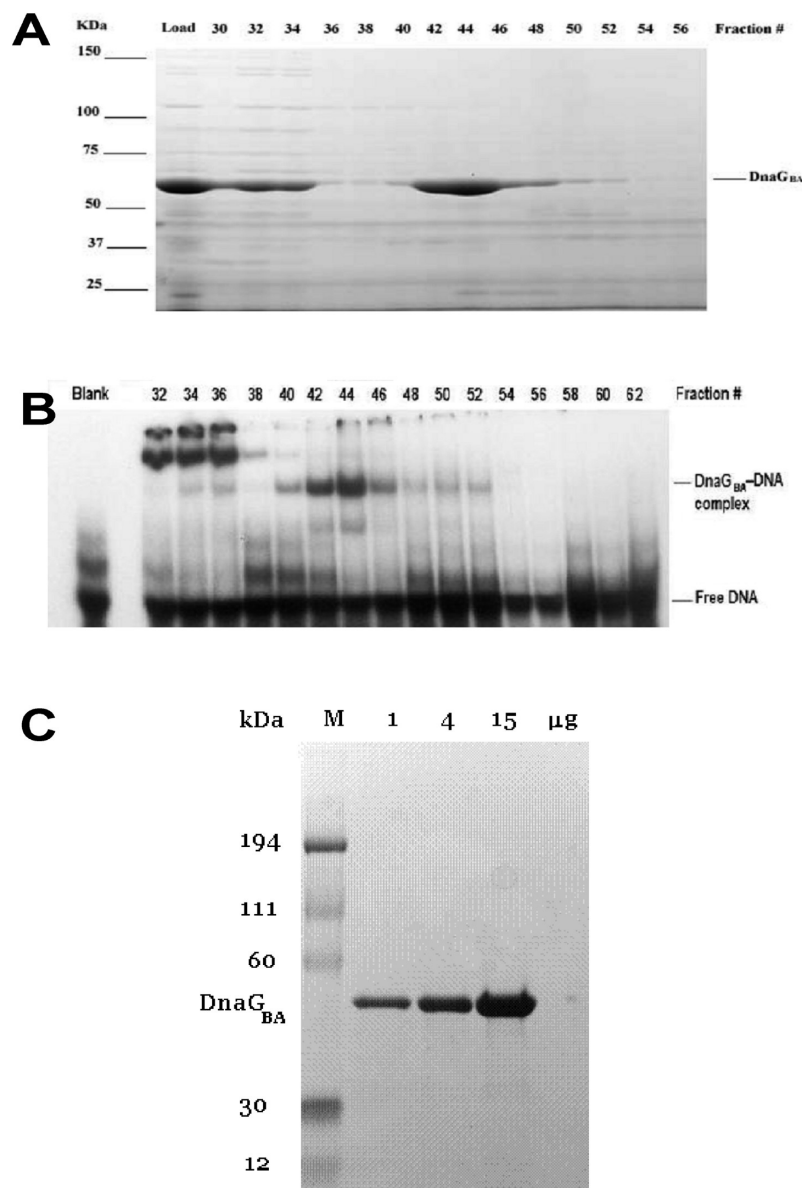


FIGURE 2: Purification and analysis of DnaG_{BA}. (A) SDS-PAGE of gel filtration fractions of DnaG_{BA} in buffer A₁₅₀ as described in Materials and Methods. (B) EMSA of DnaG_{BA} fractions using the ³²P-labeled Sixtymer oligonucleotide (Materials and Methods). (C) SDS-PAGE of DnaG_{BA} fraction V: lane 1, protein marker (M); lanes 2–4, 1, 4, and 15 μg of DnaG_{BA}, respectively.

³²P-labeled Sixtymer oligonucleotide as a probe. Active fractions, centered on the peak, were pooled and used in our studies.

DnaG_{BA} Bound ssDNA with Moderate Affinity. The first step in the mechanism of primer synthesis by DNA primases is its binding to ssDNA and formation of the DnaG_{BA}·ssDNA complex. As DNA primases prime the entire lagging strand of the genome, we anticipated that it would be able to bind to a variety of sequences with varying affinities. Therefore, we examined ssDNA binding by DnaG_{BA} using EMSA analysis. The EMSA results for ssDNA binding by DnaG_{BA} fractionated by gel filtration are presented in Figure 2B. Fractions containing DnaG_{BA} (fractions 40–46) bound the Sixtymer oligonucleotide and produced a ³²P-containing band that appeared to correspond to the DnaG_{BA}·Sixtymer complex. Thus, recombinant DnaG_{BA} appeared to be biologically active in terms of its ability to form a stable DnaG_{BA}·oligonucleotide complex that could be separated by gel electrophoresis. The SDS-PAGE analysis of purified DnaG_{BA} is shown in Figure 2C.

We have tested a variety of oligonucleotide sequences that may bind DnaG_{BA} with higher affinity. However, all of the synthetic sequences that were tested gave very similar binding affinities comparable to that described above. In addition, we explored several DNA replication origin sequences from bacteria to bacteriophages (1). Surprisingly, origin sequence derived from a single-stranded bacteriophage G4 DNA appeared to bind with higher affinity. An EMSA titration of DnaG_{BA} with a 27 bp G4ori oligonucleotide is presented in Figure 3A. Titration was conducted in a standard assay containing 0–1.6 μg of DnaG_{BA}. An increase in the level of formation of the DnaG_{BA}·G4ori complex was observed. At high primase concentrations, multiple protein–DNA complexes formed which was likely due to the process leading to the primase trimer formation. To determine quantitatively the nature of this ssDNA binding, we determined the ³²P content in each band by scintillation counting and plotted it versus the log of molar concentrations of DnaG_{BA} to create a binding isotherm (Figure 3B). The *K_d* value determined from the plot was $(3.35 \pm 0.69) \times 10^{-8}$ M, and with the Sixtymer oligonucleotide, *K_d*

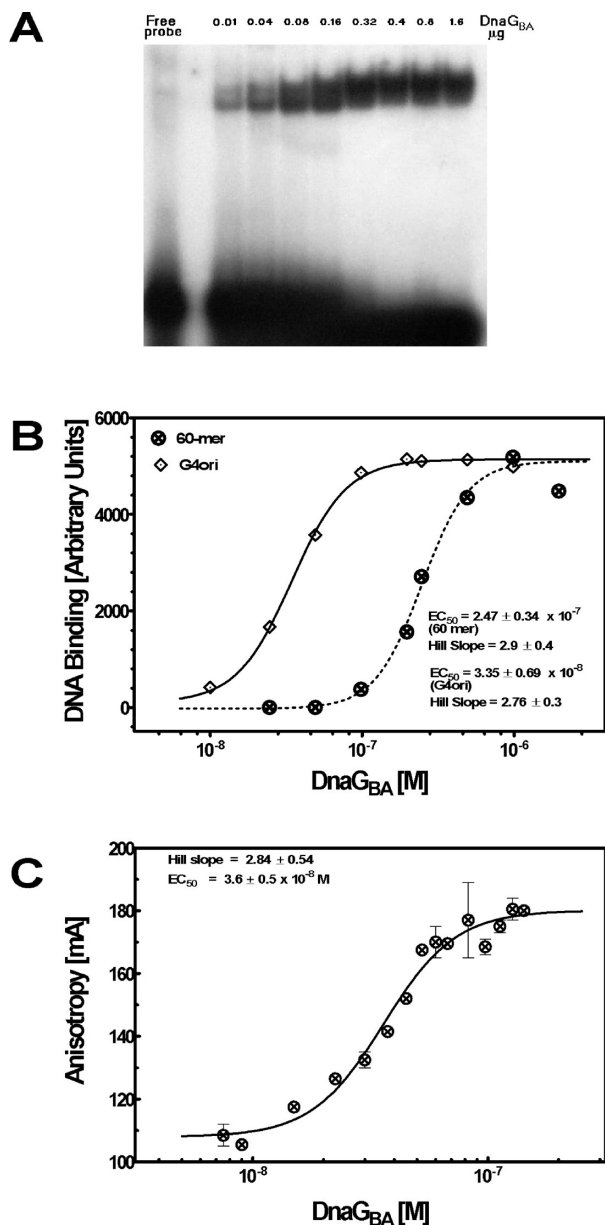


FIGURE 3: Equilibrium ssDNA binding by DnaG_{BA}. Equilibrium ssDNA binding by DnaG_{BA} was studied using G4ori and Sixtymer oligonucleotides using electrophoretic mobility shift analysis (EMSA). DNA sequences of G4ori and Sixtymer oligonucleotides are given in Materials and Methods. (A) EMSA titration of DnaG_{BA} was conducted with a ³²P-labeled G4ori oligonucleotide and titrated with DnaG_{BA} (10 ng to 1.6 μg). (B) A plot of quantitative analysis of bands in Figure 3A and its comparison with that obtained from a similar EMSA with a ³²P-labeled Sixtymer oligonucleotide (EMSA data not shown). The data points were fitted to eq 2 as described in Materials and Methods. (C) Fluorescence anisotropy analysis used for measuring ssDNA binding. DNA binding was measured using 6 nM FI-G4ori fluorescent oligonucleotide probe. Titration was conducted with DnaG_{BA}, and fluorescence anisotropy was measured as described in Materials and Methods. Anisotropy values (in milli-anisotropy or mA) were plotted vs the log of DnaG_{BA} concentration, and the plots were analyzed by nonlinear regression using Prism 5.0.

increased significantly and was 8-fold higher [$(2.47 \pm 0.34) \times 10^{-7}$ M]. The Hill slope of this plot, N_{app} , determines the numbers of protein molecules that are associating with a single ligand or, in this case, oligonucleotide. The Hill slope, as determined from this plot, was 2.76 ± 0.3 , and this value can be equated to 3. The Hill slope remained unaltered with the Sixtymer (2.9 ± 0.4). Taken together, these results indicated that DnaG_{BA} likely formed a

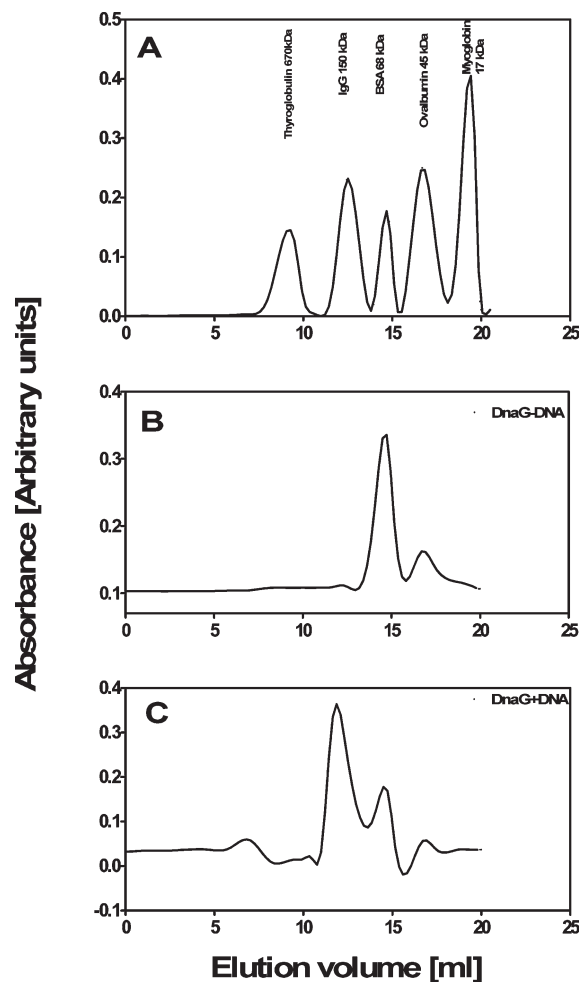


FIGURE 4: Cross-linking and gel filtration analysis of the DnaG_{BA}·DNA complex. (A) The elution profile of protein markers is shown: thyroglobulin, immunoglobulin γ, bovine serum albumin (BSA), ovalbumin, and myoglobin. (B) Elution profile of DnaG_{BA} without DNA. (C) Elution profile of the cross-linked DnaG_{BA}·DNA complex. Cross-linking and gel filtration were conducted as described in Materials and Methods.

trimer around ssDNA independent of its affinity or K_d . Our earlier studies with *E. coli* showed that DnaB and DnaG proteins formed an unstable complex with three DnaG molecules per DnaB hexamer (or DnaG₃·DnaB₆ complex) during priming.

The binding isotherm from fluorescence anisotropy titration of G4ori sequence binding is shown in Figure 3C. The data points were fitted to eq 2 using Prism 5.0. Nonlinear regression analysis gave a K_d of $(3.6 \pm 0.5) \times 10^{-8}$ M, which indicated a binding affinity at least 7-fold higher than that observed above with other oligonucleotides. The Hill slope determined from this plot was 2.84 ± 0.54 , also suggesting that DnaG_{BA} bound ssDNA as an apparent trimer. Results of the anisotropy analysis of ssDNA binding were closely comparable to that observed with the results of EMSA analysis. Therefore, both ssDNA binding analyses demonstrated that regardless of the binding affinities, DnaG_{BA} formed a trimer upon ssDNA binding.

Glutaraldehyde Cross-Linking and Gel Filtration Analysis of the DnaG_{BA}·DNA Complex. To determine the size of the DnaG_{BA}·G4ori complex, we used glutaraldehyde cross-linking followed by SEHPLC. The gel filtration column was calibrated using protein markers ranging in size from 17 to 670 kDa (Figure 4A). Purified DnaG_{BA} eluted with an apparent molecular mass of 66 ± 5 kDa (Figure 4B). We stabilized the

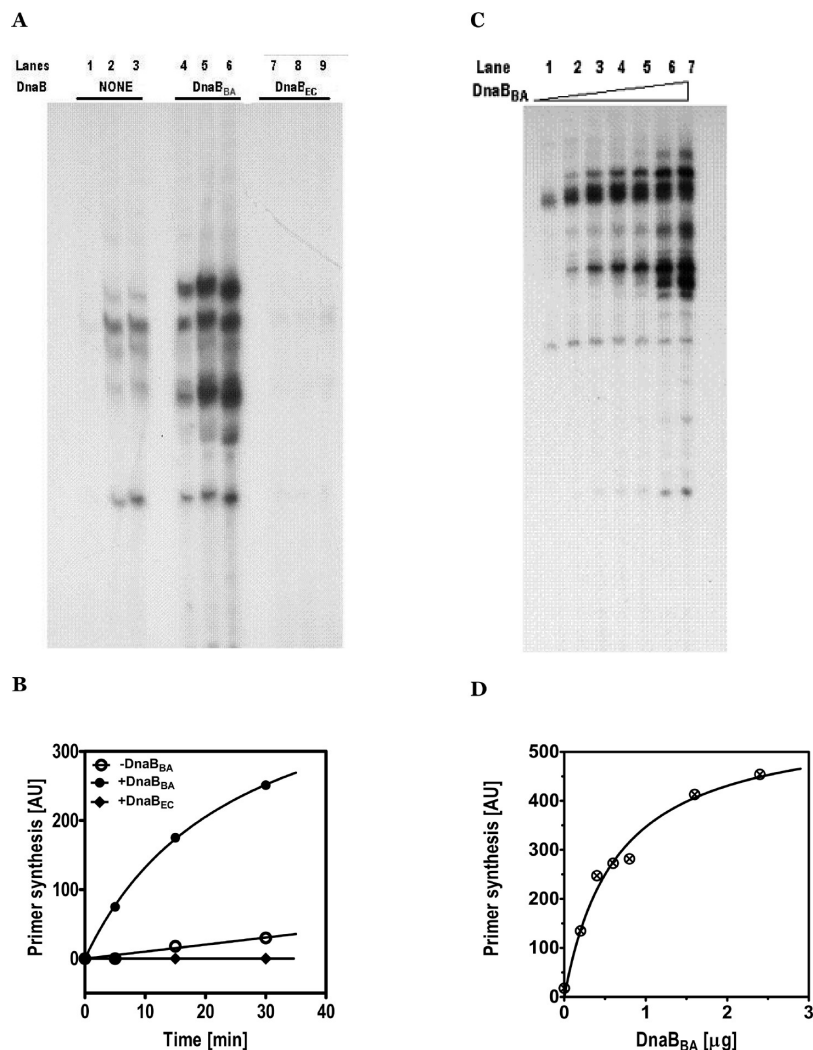


FIGURE 5: Analysis of primer synthesis by DnaG_{BA} and differential effects of DnaB_{BA} and DnaB_{EC}. Primer syntheses and analyses were conducted as described in Materials and Methods. Primers were synthesized using [³²P]dNTP. (A) Primer synthesis was conducted with 0.4 μg of DnaG_{BA}; lanes 1–3, without DnaB, for 5, 15, and 30 min, respectively; lanes 4–6, with 1.0 μg of DnaB_{BA}, for 5, 15, and 30 min, respectively; lanes 7–9, with 1.0 μg of DnaB_{EC}, for 5, 15, and 30 min, respectively. (B) Synthesized primers were quantitated by densitometric scanning. (C) Primer synthesis was conducted with 0.4 μg of DnaG_{BA} in the presence of DnaB_{BA} as follows: 0 (lane 1), 0.2 (lane 2), 0.4 (lane 3), 0.6 (lane 4), 0.8 (lane 5), 1.6 (lane 6), and 2.4 μg (lane 7). (D) Primers in panel C were quantitated as described for panel B and plotted. Data points were fitted as described in Materials and Methods.

DnaG_{BA}·G4ori complex using glutaraldehyde as a cross-linker. This is an efficient amine reactive cross-linker, which binds to the lysine residues of the proteins and creates a somewhat stable complex that can be analyzed by gel filtration. The DnaG_{BA}·G4ori complex was cross-linked with 0.2 M glutaraldehyde and was subjected to gel filtration. We found two peaks (Figure 4C). One was at a position expected for the DnaG_{BA} monomer. The second was eluted at the position from the gel filtration column earlier than DnaG_{BA} with an elution volume of ~11.5 mL. The apparent molecular mass of the complex was estimated from the linear graph derived from the plot of log[M_w] versus elution volume for protein standards and was found to be ~242 kDa. A trimeric complex, (DnaG_{BA})₃·G4ori, has a theoretical mass of ~215 kDa, and the discrepancy could be due to G4ori ssDNA and cross-linked glutaraldehyde molecules. Therefore, the gel filtration results for the cross-linked protein supported the possibility of a trimeric complex.

DNA Priming by DnaG_{BA} Was Stimulated by Anthrax DnaB Helicase but Strongly Inhibited by E. coli DnaB Helicase. The results described above demonstrate that

DnaG_{BA} is active in ssDNA binding as a trimer. Here, we have examined whether the purified DnaG_{BA} is active in primer synthesis. In the ssDNA binding studies, we have identified a sequence containing the origin of replication of bacteriophage G4 (Fl-G4ori) that DnaG_{BA} bound with high affinity. Consequently, we chose to use G4ori oligonucleotide as the substrate for analyzing primer synthesis by DnaG_{BA} in vitro.

The primer synthesis assay was used to monitor the primer synthesis from the G4ori template in the presence or absence of DnaB proteins. On the basis of the template sequence, [α-³²P]UTP was used to label the RNA primers. Primer syntheses by DnaG_{BA} alone (in the absence of DnaB proteins) were conducted for 5, 15, and 30 min. An autoradiogram of the RNA products is shown in Figure 5. The level of primer synthesis was low at 5 min, and significant amounts of RNA products were observed at both 15 and 30 min time points (Figure 5A, lanes 1–3). In general, primers were shorter than 20 nucleotides. Overall, yields of primer syntheses by DnaG_{BA} were relatively low but significant compared to those of other bacterial primases. Perhaps, its binding to ssDNA in the form of a trimer was

responsible for its higher primase activity in the absence of a DnaB effector. In the presence of DnaB_{BA}, the primase activity of DnaG_{BA} was significantly stimulated (Figure 5A, lanes 4–6). Substantial amounts of RNA products were observed at 5 min, as well as higher time points. DnaB_{BA} appeared to (i) reduce the lag time of primer synthesis and (ii) increase the rate of synthesis of primers significantly. Plots of quantitation of primer syntheses are shown in Figure 5B. In the 0–5 min range, the stimulation by DnaB_{BA} was >75-fold. At longer time points, the extent of stimulation was reduced.

The C-termini of DnaG_{BA} and other primases are less conserved compared to the N-terminal region, and it is involved in interaction with DnaB helicase. Because of the lack of homology, we anticipated that a heterologous DnaB protein like DnaB_{EC} might not have any interaction with DnaG_{BA}. To verify this notion, we examined the effects, if any, of DnaB_{EC} on the primase activity of DnaG_{BA}. The results, shown in Figure 5A (lanes 7–9), demonstrate that DnaB_{EC} likely interacted with DnaG_{BA} as DnaB_{EC} completely inhibited the primase activity of DnaG_{BA}. Consequently, it appeared that DnaG_{BA} could interact with both DnaB_{BA} and DnaB_{EC}, except that only cognate DnaB_{BA} can act as a positive effector. A titration of DnaB_{BA} in primer synthesis is shown in Figure 5C. The level of primer synthesis appeared to increase with DnaB_{BA}, pointing to a clear association between these two proteins leading to an increase in the level of priming.

DISCUSSION

Anthrax DNA Primase Is a Highly Soluble Monomeric Enzyme. DNA primases are pivotal enzymes in lagging strand DNA replication as well as in replisomes that conduct bacterial chromosomal DNA replication (1, 5, 21, 23). As described previously, DNA primase appears to form a large protein complex with hexameric DnaB protein encircling the lagging ssDNA strand in the replication fork (1, 19). Previous studies (19) indicated that this complex has a stoichiometry of three primase molecules with one DnaB protein hexamer or a 3:6 complex as shown in Figure 6. This complex regulates the site selection as well as the frequency of lagging strand priming, which in turn determines the average length of Okazaki fragments. In *E. coli*, this interaction between DnaG and DnaB proteins is quite subtle and can be demonstrated with difficulty. In addition, it is difficult to assess the interaction between DnaG protein monomers, if any, upon ssDNA binding.

Nonetheless, the *E. coli* DNA replication apparatus remains the most well-investigated system. Because of the large diversity of prokaryotes and prokaryotic pathogens, it is important to understand the mechanism of their DNA replication to develop novel strategies to combat them. Thus, it is important to determine which properties of *E. coli* DNA primase are unique only to *E. coli* versus those that are universal among prokaryotes. Except for a few recent reports, very little is known about the replication mechanism in Gram-positive bacteria. Even with the application of recombinant DNA technology, it has been difficult to study these proteins in native form because of occasional solubility problems. Surprisingly, both DnaG_{BA} and DnaB_{BA} proteins from *B. anthracis* are highly soluble in recombinant form, providing an opportunity to study these proteins in highly purified forms.

DnaG_{BA} Formed a Trimeric Complex with ssDNA. We have isolated recombinant DnaG_{BA} in highly purified form

(Figure 2C) and analyzed the mechanism of ssDNA binding. We have examined a number of synthetic DNA sequences to determine its sequence preference, if any, without success. However, an oligonucleotide with sequence derived from the origin of DNA replication of bacteriophage G4 bound DnaG_{BA} with significantly higher affinity (Figure 3) (21). With a ³²P-labeled G4ori oligonucleotide, DnaG_{BA} bound with high affinity (Figure 3). The K_d value determined from the binding isotherm was $(3.35 \pm 0.69) \times 10^{-8}$ M. In addition, the Hill coefficient, N_{app} , derived from the nonlinear regression (eq 2) was 2.76 ± 0.3 (Figure 3B). Therefore, DnaG_{BA} appears to form a trimer during ssDNA binding even though it is monomeric in solution (Figure 2). *E. coli* primase, DnaB_{EC}, is not known to form such a trimer alone, but it forms a trimer in a complex with a DnaB hexamer (19).

Fluorescein-labeled 27 bp G4 origin sequence, Fl-G4ori, was used to quantitate its binding to DnaG_{BA} using fluorescence anisotropy as a second method of analysis. The K_d was $(3.6 \pm 0.5) \times 10^{-8}$ M, which indicated a binding affinity 7-fold higher than that observed above with other oligonucleotides. Even with the G4ori sequence and higher-affinity binding, the Hill coefficient was 2.84 ± 0.54 which can be approximated to 3, which also showed that DnaG_{BA} bound the oligonucleotide as a trimer. Therefore, both analyses (Figure 2B,C) appeared to demonstrate that regardless of the binding affinities, DnaG_{BA} appeared to form a trimer upon ssDNA binding. Thus, it could be a distinguishing feature of DnaG_{BA} in that it appeared to form a trimer with ssDNA, independent of DnaB protein.

A DnaG_{BA}·G4ori complex, cross-linked with glutaraldehyde and the size of the cross-linked complex, was analyzed by SEHPLC (Figure 4). SEHPLC and determination of the molecular mass of the complex indicated a mass of 242 kDa for the cross-linked complex, indicating a 3.4:1 DnaG_{BA}·G4ori ratio in the complex that could be approximated to a trimeric complex. Thus, it appeared that one of the distinguishing features of DnaG_{BA} is its ability to form a trimer, presumably a toroidal trimeric ring, around ssDNA, in a manner independent of DnaB protein. The alternative scenario, three primases binding sequentially to three separate sites on one oligonucleotide, seems unlikely due to the small size (27 bp) of the oligonucleotide, and in addition, the binding kinetics does not support this mechanism. In addition, primases are known to interact structurally with DnaB helicases in the replication fork. Because of the toroidal structure of DnaB helicase, this process would require formation of a toroidal ring (19, 33). In this respect, DNA primase purified from high-temperature bacterium, DnaG_{BS}, appears to form a stable complex with its cognate DnaB_{BS} (32). This complex contains three DnaG_{BS} molecules per DnaB hexamer. Bailey et al. resolved the structure of a complex DnaB_{BS} with the helix binding domain of DnaG_{BS} with a 6:3 ratio (33). However, it is not known whether it can bind ssDNA alone and form a trimer with ssDNA.

Primer Synthesis by DnaG_{BA} Was Stimulated by Anthrax DnaB Helicase and Inhibited by E. coli DnaB Helicase. DnaG_{BA} synthesized RNA primers on the G4ori template in the absence of DnaB_{BA} protein (Figure 5A). However, the rate of primer synthesis was low (Figure 5B). DnaB_{BA} significantly stimulated the rate as well as the extent of primer synthesis. In the initial stage, the stimulation by DnaB_{BA} was ≥75-fold. Beyond this initial stage, the extent of stimulation was reduced as expected. In addition to the stimulation of the rate of primer synthesis, the average size of the primers was also increased and a greater size

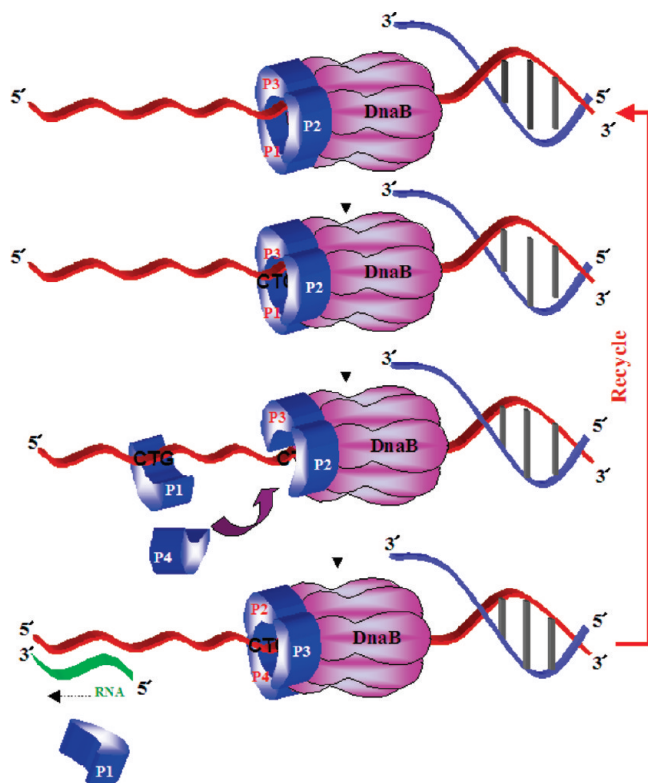


FIGURE 6: Primase recycling model of distributive RNA priming. (1) We have considered here a $(\text{DnaG})_3 \cdot (\text{DnaB})_6$ complex formed from one DnaB hexamer and three DnaG primase monomers (P1–P3). (2) One monomer (P1) identifies and binds to a preferred sequence with a slightly higher affinity, breaks off from the complex, and initiates primer synthesis. (3) A free primase monomer (P4) fills the vacant position in the $(\text{DnaG})_3 \cdot (\text{DnaB})_6$ complex. (4) Primase molecule (P1) completes primer synthesis and dissociates from the primed lagging strand and a new cycle of priming begins.

distribution of RNA primers was observed (Figure 5A,C). A titration of DnaB_{BA} in a primer synthesis assay indicated that DnaB_{BA} stimulated RNA synthesis by DnaG_{BA} in a dose-dependent manner (Figure 5D). The amount of DnaG_{BA} in each assay was $0.4 \mu\text{g}$, and half-maximal RNA synthesis was observed at $0.6 \mu\text{g}$ of DnaB_{BA} . The amount of DnaB_{BA} needed to reach the half-maximal synthesis appeared to be somewhat greater than that anticipated from a complex containing three DnaG_{BA} monomers and one DnaB_{BA} hexamer. However, this could be due to weaker interaction between the two enzymes requiring a higher level of DnaB_{BA} to form the $(\text{DnaG}_{\text{BA}})_3 \cdot (\text{DnaB}_{\text{BA}})_6$ complex.

We also examined the effect of a heterologous DnaB, DnaB_{EC} , on the primer synthesis by DnaG_{BA} . The functional interaction between DnaB and primase involves the last 16 amino acid residues of the C-terminal region of the primase (41) and the N-terminal 12 kDa domain of the DNA helicase, corresponding to amino acids residues 14–136 (43). Considering the fact that the C-terminal DnaB binding region of DnaG_{BA} is different from that of *E. coli* DnaG_{EC} (Figure 1), any significant interaction as well as a change in primer synthesis due to DnaB_{EC} was not anticipated. Surprisingly, as shown in Figure 5A, DnaB_{EC} completely inhibited primer synthesis by DnaG_{BA} . Thus, even with significant sequence heterogeneity, DnaB_{EC} and DnaG_{BA} appeared to interact functionally or physically, and this interaction led to inhibition of the primase activity of DnaG_{BA} . Therefore, homologous DnaB_{BA} acted as a positive effector of DnaG_{BA} , whereas heterologous DnaB_{EC} acted as a negative

effector. On the basis of the results presented here as well as previous studies on DNA primases, as discussed above, we propose a hypothetical model for the distributive priming of the lagging strand of bacterial replication forks (Figure 6). The functional $\text{DnaB} \cdot \text{DnaG}$ complex binds to the lagging strand with a 6:3 subunit ratio. Once an appropriate DNA sequence comes in contact with a primase subunit of the $\text{DnaB} \cdot \text{DnaG}$ complex, it binds to the ssDNA with higher affinity. The higher-affinity binding forces it to break off from the complex as a monomer, and it leaves a gap in the primase trimeric ring. This monomeric primase then synthesizes the primer. In the meantime, a new primase monomer joins the $\text{DnaB} \cdot \text{DnaG}$ assembly to fill the gap in the trimeric primase ring, thereby restoring the 6:3 complex, and it starts a new cycle of priming. In this model, DNA primase continually recycles and the priming does not impede the movement of the replisome powered by DnaB helicase. Further studies are required to dissect the proposed model in Figure 6.

ACKNOWLEDGMENT

We thank various colleagues for discussions and helpful suggestions, members of the Biswas laboratory for technical assistance, and Ms. Anu Singh, Julia Crawford, and Dr. John Pastorino for editing the manuscript.

REFERENCES

- Kornberg, A., and Baker, T. A. (1992) DNA Replication, W. H. Freeman and Co., New York.
- DePamphilis, M. L. (1998) Initiation of DNA replication in eukaryotic chromosomes. *J. Cell. Biochem. Suppl.* 30–31, 8–17.
- Datta, H. J., Khatri, G. S., and Bastia, D. (1999) Mechanism of recruitment of DnaB helicase to the replication origin of the plasmid pSC101. *Proc. Natl. Acad. Sci. U.S.A.* 96, 73–78.
- Bramhill, D., and Kornberg, A. (1988) Duplex opening by dnaA protein at novel sequences in initiation of replication at the origin of the *E. coli* chromosome. *Cell* 52, 743–755.
- Bramhill, D., and Kornberg, A. (1988) A model for initiation at origins of DNA replication. *Cell* 54, 915–918.
- Fuller, R. S., and Kornberg, A. (1983) Purified dnaA protein in initiation of replication at the *Escherichia coli* chromosomal origin of replication. *Proc. Natl. Acad. Sci. U.S.A.* 80, 5817–5821.
- Biswas, E. E., Biswas, S. B., and Bishop, J. E. (1986) The dnaB protein of *Escherichia coli*: Mechanism of nucleotide binding, hydrolysis, and modulation by dnaC protein. *Biochemistry* 25, 7368–7374.
- Biswas, S. B., and Biswas, E. E. (1987) Regulation of dnaB function in DNA replication in *Escherichia coli* by dnaC and lambda P gene products. *J. Biol. Chem.* 262, 7831–7838.
- Wickner, S., and Hurwitz, J. (1975) Interaction of *Escherichia coli* dnaB and dnaC(D) gene products in vitro. *Proc. Natl. Acad. Sci. U.S.A.* 72, 921–925.
- Biswas, S. B., and Biswas-Fiss, E. E. (2006) Quantitative analysis of binding of single-stranded DNA by *Escherichia coli* DnaB helicase and the $\text{DnaB} \cdot \text{DnaC}$ complex. *Biochemistry* 45, 11505–11513.
- Gaylo, P. J., Turjman, N., and Bastia, D. (1987) DnaA protein is required for replication of the minimal replicon of the broad-host-range plasmid RK2 in *Escherichia coli*. *J. Bacteriol.* 169, 4703–4709.
- Konieczny, I., and Helinski, D. R. (1997) Helicase delivery and activation by DnaA and TrfA proteins during the initiation of replication of the broad host range plasmid RK2. *J. Biol. Chem.* 272, 33312–33318.
- Zhong, Z., Helinski, D., and Toukdarian, A. (2003) A specific region in the N terminus of a replication initiation protein of plasmid RK2 is required for recruitment of *Pseudomonas aeruginosa* DnaB helicase to the plasmid origin. *J. Biol. Chem.* 278, 45305–45310.
- Alfano, C., and McMacken, R. (1989) Ordered assembly of nucleoprotein structures at the bacteriophage lambda replication origin during the initiation of DNA replication. *J. Biol. Chem.* 264, 10699–10708.
- Dodson, M., Roberts, J., McMacken, R., and Echols, H. (1985) Specialized nucleoprotein structures at the origin of replication of bacteriophage lambda: Complexes with lambda O protein and with

- lambda O, lambda P, and *Escherichia coli* DnaB proteins. *Proc. Natl. Acad. Sci. U.S.A.* 82, 4678–4682.
16. Alfano, C., and McMacken, R. (1988) The role of template super-helicity in the initiation of bacteriophage lambda DNA replication. *Nucleic Acids Res.* 16, 9611–9630.
 17. Dodson, M., Echols, H., Wickner, S., Alfano, C., Mensa-Wilmot, K., Gomes, B., LeBowitz, J., Roberts, J. D., and McMacken, R. (1986) Specialized nucleoprotein structures at the origin of replication of bacteriophage lambda: Localized unwinding of duplex DNA by a six-protein reaction. *Proc. Natl. Acad. Sci. U.S.A.* 83, 7638–7642.
 18. Arai, K., and Kornberg, A. (1979) A general priming system employing only dnaB protein and primase for DNA replication. *Proc. Natl. Acad. Sci. U.S.A.* 76, 4308–4312.
 19. Mitkova, A. V., Khopde, S. M., and Biswas, S. B. (2003) Mechanism and stoichiometry of interaction of DnaG primase with DnaB helicase of *Escherichia coli* in RNA primer synthesis. *J. Biol. Chem.* 278, 52253–52261.
 20. Stayton, M. M., Bertsch, L., Biswas, S., Burgers, P., Dixon, N., Flynn, J. E., Fuller, R., Kaguni, J., Kabori, J., Kodaira, M., Low, R., and Kornberg, A. (1983) Enzymatic recognition of DNA replication origins. *Cold Spring Harbor Symp. Quant. Biol.* 47 (Part 2), 693–700.
 21. Stayton, M. M., and Kornberg, A. (1983) Complexes of *Escherichia coli* primase with the replication origin of G4 phage DNA. *J. Biol. Chem.* 258, 13205–13212.
 22. Sugino, A., Hirose, S., and Okazaki, R. (1972) RNA-linked nascent DNA fragments in *Escherichia coli*. *Proc. Natl. Acad. Sci. U.S.A.* 69, 1863–1867.
 23. Arai, K., Low, R. L., and Kornberg, A. (1981) Movement and site selection for priming by the primosome in phage phi X174 DNA replication. *Proc. Natl. Acad. Sci. U.S.A.* 78, 707–711.
 24. Lu, Y. B., Ratnakar, P. V., Mohanty, B. K., and Bastia, D. (1996) Direct physical interaction between DnaG primase and DnaB helicase of *Escherichia coli* is necessary for optimal synthesis of primer RNA. *Proc. Natl. Acad. Sci. U.S.A.* 93, 12902–12907.
 25. Yoda, K., and Okazaki, T. (1991) Specificity of recognition sequence for *Escherichia coli* primase. *Mol. Gen. Genet.* 227, 1–8.
 26. Yoda, K., Yasuda, H., Jiang, X. W., and Okazaki, T. (1988) RNA-primed initiation sites of DNA replication in the origin region of bacteriophage lambda genome. *Nucleic Acids Res.* 16, 6531–6546.
 27. Tomasz, A. (1994) Multiple-antibiotic-resistant pathogenic bacteria. A report on the Rockefeller University Workshop. *N. Engl. J. Med.* 330, 1247–1251.
 28. Read, T. D., Peterson, S. N., Tourasse, N., Baillie, L. W., Paulsen, I. T., Nelson, K. E., Tettelin, H., Fouts, D. E., Eisen, J. A., Gill, S. R., Holtzapple, E. K., Okstad, O. A., Helgason, E., Rilstone, J., Wu, M., Kolonay, J. F., Beanan, M. J., Dodson, R. J., Brinkac, L. M., Gwinn, M., DeBoy, R. T., Madpu, R., Daugherty, S. C., Durkin, A. S., Haft, D. H., Nelson, W. C., Peterson, J. D., Pop, M., Khouri, H. M., Radune, D., Benton, J. L., Mahamoud, Y., Jiang, L., Hance, I. R., Weidman, J. F., Berry, K. J., Plaut, R. D., Wolf, A. M., Watkins, K. L., Niernan, W. C., Hazen, A., Cline, R., Redmond, C., Thwaite, J. E., White, O., Salzberg, S. L., Thomason, B., Friedlander, A. M., Koehler, T. M., Hanna, P. C., Kolsto, A. B., and Fraser, C. M. (2003) The genome sequence of *Bacillus anthracis* Ames and comparison to closely related bacteria. *Nature* 423, 81–86.
 29. Takami, H., Nakasone, K., Takaki, Y., Maeno, G., Sasaki, R., Masui, N., Fuji, F., Hirama, C., Nakamura, Y., Ogasawara, N., Kuhara, S., and Horikoshi, K. (2000) Complete genome sequence of the alkaliphilic bacterium *Bacillus halodurans* and genomic sequence comparison with *Bacillus subtilis*. *Nucleic Acids Res.* 28, 4317–4331.
 30. Koepsell, S. A., Larson, M. A., Griep, M. A., and Hinrichs, S. H. (2006) *Staphylococcus aureus* helicase but not *Escherichia coli* helicase stimulates *S. aureus* primase activity and maintains initiation specificity. *J. Bacteriol.* 188, 4673–4680.
 31. Koepsell, S. A., Larson, M. A., Frey, C. A., Hinrichs, S. H., and Griep, M. A. (2008) *Staphylococcus aureus* primase has higher initiation specificity, interacts with single-stranded DNA stronger, but is less stimulated by its helicase than *Escherichia coli* primase. *Mol. Microbiol.* 68, 1570–1582.
 32. Bird, L. E., Pan, H., Soultanas, P., and Wigley, D. B. (2000) Mapping protein-protein interactions within a stable complex of DNA primase and DnaB helicase from *Bacillus stearothermophilus*. *Biochemistry* 39, 171–182.
 33. Bailey, S., Eliason, W. K., and Steitz, T. A. (2007) Structure of hexameric DnaB helicase and its complex with a domain of DnaG primase. *Science* 318, 459–463.
 34. Biswas, E. E., and Biswas, S. B. (1999) Mechanism of DNA binding by the DnaB helicase of *Escherichia coli*: Analysis of the roles of domain γ in DNA binding. *Biochemistry* 38, 10929–10939.
 35. Gryczynski, I., Gryczynski, Z., and Lakowicz, J. R. (1998) Fluorescence anisotropy controlled by light quenching. *Photochem. Photobiol.* 67, 641–646.
 36. Maag, D., Fekete, C. A., Gryczynski, Z., and Lorsch, J. R. (2005) A conformational change in the eukaryotic translation preinitiation complex and release of eIF1 signal recognition of the start codon. *Mol. Cell* 17, 265–275.
 37. Sarkar, P., Bharill, S., Gryczynski, I., Gryczynski, Z., Nair, M. P., and Lacko, A. G. (2008) Binding of 8-anilino-1-naphthalenesulfonate to lecithin:cholesterol acyltransferase studied by fluorescence techniques. *J. Photochem. Photobiol., B* 92, 19–23.
 38. Lakowicz, J. R. (1999) Principles of fluorescence spectroscopy, 2nd ed., Plenum Publishers, New York.
 39. Khopde, S., Biswas, E., and Biswas, S. (2002) Affinity and sequence specificity of DNA binding and site selection for primer synthesis by *Escherichia coli* primase. *Biochemistry* 41, 14820–14830.
 40. Masai, H., Nomura, N., and Arai, K. (1990) The ABC-primosome. A novel priming system employing dnaA, dnaB, dnaC, and primase on a hairpin containing a dnaA box sequence. *J. Biol. Chem.* 265, 15134–15144.
 41. Tougu, K., and Mariani, K. J. (1996) The extreme C terminus of primase is required for interaction with DnaB at the replication fork. *J. Biol. Chem.* 271, 21391–21397.
 42. Tougu, K., Peng, H., and Mariani, K. J. (1994) Identification of a domain of *Escherichia coli* primase required for functional interaction with the DnaB helicase at the replication fork. *J. Biol. Chem.* 269, 4675–4682.
 43. Nakayama, N., Arai, N., Kaziro, Y., and Arai, K. (1984) Structural and functional studies of the dnaB protein using limited proteolysis. Characterization of domains for DNA-dependent ATP hydrolysis and for protein association in the primosome. *J. Biol. Chem.* 259, 88–96.